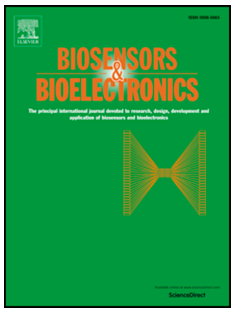

One-step modification of nano-polyaniline/glucose oxidase on double-side printed flexible electrode for continuous glucose monitoring: Characterization, cytotoxicity evaluation and in vivo experiment

Yu Cai, Bo Liang, Shidie Chen, Qin Zhu, Tingting Tu, Ke Wu, Qingpeng Cao, Lu Fang, Xiao Liang, Xuesong Ye

PII: S0956-5663(20)30402-4

DOI: https://doi.org/10.1016/j.bios.2020.112408

Reference: BIOS 112408

To appear in: *Biosensors and Bioelectronics*

Received Date: 15 March 2020

Revised Date: 5 June 2020

Accepted Date: 21 June 2020

Please cite this article as: Cai, Y., Liang, B., Chen, S., Zhu, Q., Tu, T., Wu, K., Cao, Q., Fang, L., Liang, X., Ye, X., One-step modification of nano-polyaniline/glucose oxidase on double-side printed flexible electrode for continuous glucose monitoring: Characterization, cytotoxicity evaluation and in vivo experiment, *Biosensors and Bioelectronics* (2020), doi: https://doi.org/10.1016/j.bios.2020.112408.

CRediT author statement

Yu Cai: Conceptualization, Methodology, Software, Visualization, Writing-Original Draft.

Bo Liang: Writing-Review & Editing, Supervision, Funding acquisition.

Shidie Chen: Validation, Data Curation.

Qin Zhu: Writing-Review & Editing.

TingtingTu: Investigation, Resources.

Ke Wu: Investigation.

Qingpeng Cao: Writing-Review & Editing.

Lu Fang: Writing-Review & Editing.

Xiao Liang: Investigation.

Xuesong Ye: Project administration, Funding acquisition.

One-step Modification of Nano-polyaniline/glucose oxidase on Double-side Printed Flexible Electrode for Continuous Glucose Monitoring: Characterization, Cytotoxicity Evaluation and in vivo Experiment

Yu Cai [a], Bo Liang [a*], Shidie Chen [a], Qin Zhu [a], Tingting Tu [a], Ke Wu [b], Qingpeng Cao [a], Lu Fang [c], Xiao Liang [b], Xuesong Ye [a*]

[a] Biosensor National Special Laboratory, Key Laboratory of Biomedical Engineering of Ministry of Education, College of Biomedical Engineering and Instrument Science, Innovation Center for Minimally Invasive Technique and Device, Zhejiang University, Zhejiang University, Hangzhou 310027, PR China.

[b] Key Lab of Surgery of Zhejiang Province, Sir Run Run Shaw Hospital, Zhejiang University, Hangzhou310027, PR China

[c] College of Automation, Hangzhou Dianzi University, Hangzhou 310018, PR China.

[*]Corresponding author. Tel: +86 571 87952756

E-mail address: yexuesong@zju.edu.cn (X. Ye), boliang1986@zju.edu.cn (B. Liang)

Abstract

The single-step modification of the nanostructured polyaniline (PANI)/glucose oxidase (GOD) enzyme on double-sided, screen-printed, flexible electrodes doped with Prussian blue (PB), has been achieved and successfully applied in continuous glucose monitoring in vivo, and its biocompatibility has been evaluated systematically. The proposed fabrication procedure is simple, low cost, and suitable for large-scale production. PB doped with carbon ink catalyzes the reduction of hydrogen peroxide (H_2O_2) in low-voltage conditions, which could help eliminate interferences. And the PANI/GOD nanostructure makes the GOD enzyme more stable for long-term, in vivo monitoring. More importantly, a polyurethane (PU) layer is deposited on the electrode's surface as a diffusion limiting membrane that enhanced the linear range and biocompatibility. In tests in vitro, the proposed biosensor achieved a linear range of 0–12mM and a good sensitivity of 16.66 $uA \cdot mM^{-1} \cdot cm^{-2}$(correlation coefficient R^2= 0.9962) with an excellent specificity to glucose. The biosensor exhibits long-term stability, with a maximum lifespan of 14 days when stored in phosphate buffer solution at 4°C, and achieves a sensitivity of 120%. The biocompatibilities of the electrode materials have also been systematically evaluated in cytotoxicity and cell adhesion tests to ensure the safety of implantation. In experiments in vivo, the biosensor can successfully monitor the glucose level fluctuation of rats after 24 hours following implantation. Overall, the biosensor fabricated with the double-side, screen-printing process, satisfies the glucose monitoring range in vivo and eliminates various types of interference, thus establishing a new, large-scale production procedure for flexible in vivo biosensors.

***KEYWORDS*:** Glucose biosensor; Prussian blue; Polyaniline; Screen-printed electrode; Cytotoxicity; Implantable sensor.

1. Introduction

Diabetes mellitus is a metabolic disease that has been recognized as a worldwide public health problem. It can cause many complications, such as hypertension, kidney failure, heart disease, and blindness (Liang et al. 2013; Wang 2008). Fortunately, continuous glucose monitoring systems (CGMSs) provide an effective, real-time, and long-term self-monitoring method for diabetic therapy. Several commercial CGMS products and newly developed systems have been developed (Kim et al. 2019). However, there are still several problems associated with CGMS, such as interference, mechanical friction, and biocompatibility evaluation when these systems are implanted in the human body. Active substances present in the interstitial fluid can directly react on invasive electrodes that cause errors in the final signal. Mechanical friction on the electrode layer induced when devices are worn leads to electrode failure (He et al. 2016). The biocompatibility and cytotoxicity of invasive electrodes are also significant but have not been investigated in detail. It is thus important that these attributes are evaluated before electrodes are used in practical applications.

CGMS sensors work in biological tissues, and will be affected by active substances in the interstitial fluid. Strategies employed to avoid interference have been studied and have involved the immobilization of mediators with the GOD enzyme. These mediators have a lower oxidation potential, and facilitate electron transfer by rapidly shuttling electrons between the enzyme and electrode, thus decreasing the detection potential of the sensor (Kim et al. 2019). Many mediator types have been studied, including graphene, metal–organic, and electron (Cinti et al. 2018; Kim et al. 2019; Kwak et al. 2012; Xu et al. 2015; Zeng et al. 2011; Zhang et al. 2004). Among these, Prussian blue (PB) has been extensively used. PB could catalyze the reduction of hydrogen peroxide at a very low voltage, and could avoid the interference of ascorbic acid, dopamine, and lactic acid when applied to in vivo monitoring (Karyakin et al. 2000; Nossol and Zarbin 2009; Xu et al. 2015; Zhang et al. 2004). Compared with electrochemical deposition, PB modified with screen-printing is more stable and has an improved anti-interference performance. Therefore, herein, screen-printing with PB-doped carbon ink is explored for CGMS.

Conventional invasive metallic electrodes are extensively used, but they are stiff, complicated, and costly (Fang et al. 2014; Fang et al. 2018). Rigid structures cause mechanical friction after implantation (flexible materials also but eventually less), and users also suffer pain and discomfort and bear a large economic burden that restricts the applications of CGMS. For this reason, flexible invasive electrodes are studied instead, such as screen-printed electrodes that have been used in the FreeStyle Navigator (Abbot, Abbot Park, IL, USA) (Yoo and Lee 2010), and in other invasive biosensors (Kim et al. 2019; Ling et al. 2018; Nguyen et al. 2019). Screen-printed electrodes are flexible, can match the deformation of tissue, and ease user discomfort. Otherwise, screen-printed electrodes are easily fabricated with rapid

prototyping that makes mass production possible. However, the structure of previous screen-printed biosensors is not suitable for implantation. Thus, a double-sided screen-printing is applied in this study to reduce the electrode size for a better implantation.

The biocompatibility of CGMS is very important. Many biocompatible materials have been introduced as protective coatings, including chitosan and polyurethane (PU). These two materials can significantly improve the biocompatibility of the modified objects (Fang et al. 2017; Shin et al. 2004; Yu et al. 2006). Nevertheless, a limited number of research studies have focused on the materials of screen-printed electrodes, like carbon or insulating ink. Most of these materials contain organic polymers that may be toxic to humans. Previous studies only focused on the biocompatibility of single layers or materials, but not on the entire electrode system that is necessary for practical applications. Accordingly, the cytotoxicity of all the constituent materials of our glucose biosensors are systematically evaluated in this study in the effort to guarantee safe use after implantation.

Correspondingly, in this study, we develop a single-step modification process for a nanostructured polyaniline (PANI)/glucose oxidase (GOD) enzyme biosensor based on flexible PB-doped, double-sided, screen-printed electrodes. Our glucose biosensors use flexible, double-sided, screen-printed electrodes that consist of PB-doped carbon ink as a working electrode and Ag/AgCl ink as the counter electrode. Furthermore, we synthesize solid PANI powder and mix it with (GOD) to form a nano-PANI/GOD structure (Kausar 2019; Shoaie et al. 2019). This single-step modification simplifies the fabrication process and structure of the glucose biosensor. A PU membrane was employed as a protective coating to limit the diffusion of glucose and improve biocompatibility. Before implantation, we designed several experiments to evaluate the biocompatibility of our electrode in vitro and validated the safety of the biosensor. Finally, the biosensor was applied in experiments in vivo based on which we successfully monitored the glucose levels in rats after a 24 hours implantation period.

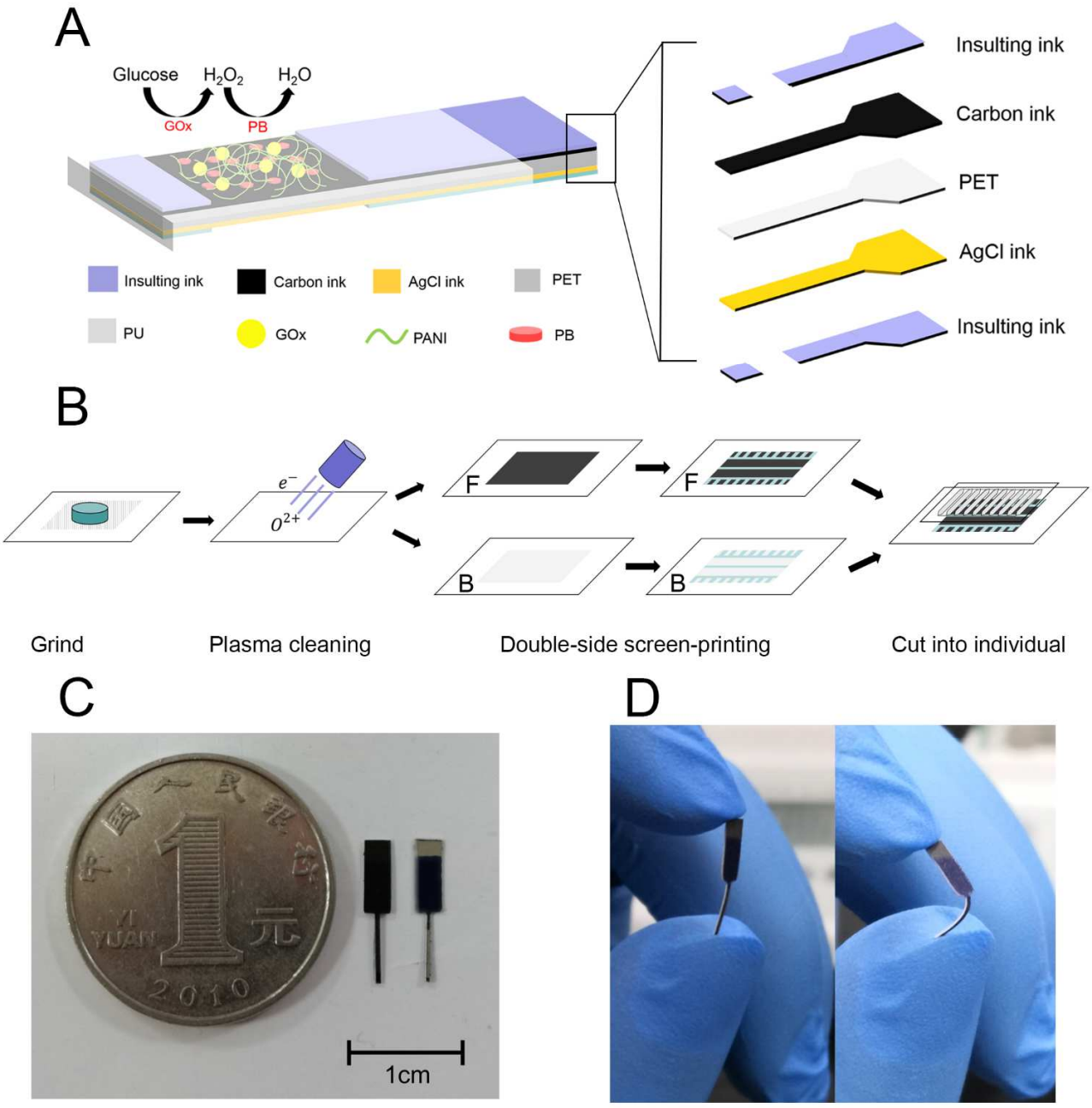

Fig. 1 (A) Glucose sensor structure composed of polyethylene terephthalate (PET) substrate, Prussian blue (PB)-doped working electrode, Ag/AgCl counter electrode, and the insulating area. (B) The electrode is printed on both sides and is cut to form individual electrodes. (C) The individual electrodes are 25mm in length and 0.5 mm in width. (D) Photographs of the electrode before and after bending at an angle of 90°.

2. Material and methods

2.1 Reagents

Polyethylene terephthalate (PET) film was purchased from Qicheng. PB-doped carbon ink and Ag/AgCl ink were purchased from the Gwent Group Ltd. GOD from Aspergillus Niger (>180 unitsmg^{-1} protein), dimethylformamide (DMF), tetrahydrofuran (THF), ascorbic acid (AA), dopamine (DA), and

uric acid (UA),were purchased from Aladdin Ltd. (Shanghai, China). Aniline, HCl (36%), ammonium persulphate, glutaraldehyde (25%), lactic acid (LA), NaCl, glucose, and bovine serum albumin (BSA), were purchased from Sinopharnm Chemical Reagent Co. Ltd. (China). PU was purchased from Sigma Co. GOD (30 mg·mL^{-1}) and BSA (10 mg mL^{-1}) were prepared in 0.01 M phosphate buffer solution (PBS, pH=7.4). The 3-(4, 5-dimethylthiazol-2-yl)-2, 5-diphenyl tetrazolium bromide (MTT) array kit and polyurethane were purchased from Sigma Co. PBS (pH=7.4), and Dublecco's modified eagle medium (DMEM)was purchased from Genom Ltd. (Hangzhou). FPS and trypsin were purchased from Thermo Fisher Scientific Ltd. All aqueous solutions were prepared with deionized water.

2.2 Apparatus

The morphologies and structures of the modified screen-printed electrodes were characterized with a field emission scanning electron microscope (FESEM, Hitachi SU8010). All electrochemical measurements are performed with an IVIUM CompacStat.h electrochemical workstation. The surface morphological studies were conducted with the thermal field emission scanning electron microscope (FSEM), SIRON-100 (FEI, USA). The EDS spectrum was obtained with the FSEM that was equipped with an energy-dispersive X-ray spectrometer (EDS) (GENESIS4000, EDAX, USA).

2.3 Preparation and fabrication of screen-printed electrode

The fabrication of the screen-printed electrode is shown in Fig. 1B. Firstly, the PET sheets are ground with a cylinder sandpaper to get a rough surface (first graphic in Fig. 1B). Then they are cleaned by oxygen plasma (second graphic in Fig. 1B). The next step is printing of carbon and Ag/AgCl conductive ink onto a PET film (thickness = 200 μm). The carbon conductive ink was doped with PB before screen-printing. In comparison with other screen-printed electrodes, this film was printed on both sides. One side was printed with PB-doped carbon conductive ink as the working electrode. The other side was printed with Ag/AgCl conductive ink as the counter electrode (the third graphic in Fig. 1B). The front side was first printed with carbon ink as the working electrode and the other side was then printed with Ag/AgCl ink as the counter electrode. After printing the working and counter electrode areas, the film was printed with insulating ink to form a different electrode area (the fourth graphic in Fig. 1B). All of the printed layers were subjected to the curing process at 90°C for 10 min. Finally, the screen-printed film was cut by the cutting machine to form individual electrodes (the fifth graphic in Fig. 1B). The cutting pattern was designed a priori and each film was cut in 20 individual electrodes.

2.4 Modification of glucose biosensor

Fabrication of solid PANI powder: Firstly, 1.4 mL aniline was added to 25 mL of 1 M hydrochloric acid solution with vigorous stirring. Subsequently, 2.0 mg ammonium peroxydisulfate was added to the

mixture at a slow pace, and was stirred for 3 h at 20°C until the reaction was completed. Ammonium peroxydisulfate can oxidize aniline to form PANI. Finally, the precipitation was collected by sucking filtration with a 0.22 μm membrane, and was rinsed with deionized water until the filtrate became colorless. It was then dried in a vacuum oven at 50°C for 24 h to obtain a dark green PANI powder.

Preparation of PANI/GOD mixed solution A: 30 mg PANI powder synthesized before was added to 1 mL of PBS solution (0.01 M, pH = 7.4) via ultrasonication to obtain a dark green PANI solution. B solution: GOD enzyme (30 mg) and BSA (10 mg) were added to 1 mL of PBS (0.01 M, pH = 7.4). Solutions A and B were mixed uniformly at a proportion of 2:1 and stored at 4°C for subsequent use.

Fabrication of the glucose biosensor and immobilization of glucose oxidase enzyme: Firstly, the fabricated screen-printed electrode was electrochemically cleaned via cyclic voltammetry (CV) in 1 M H_2SO_4 between -0.4 V and 0.6 V at 50 mV/s for 5 cycles, and was rinsed with deionized water. Subsequently, 5 μL of the mixed PANI/GOD solutions prepared just before, was dropped in the area of the working and dried at room temperature for 6 h. The electrode was then crosslinked by glutaraldehyde (25%) for 90 min at 37°C. Finally, the electrode was covered with PU membranes with 1.5% PU (solution of 98% Tetrahydrofuran + 2% Dimethylformamide, contain 1.5% PU).

2.5 In vitro evaluation and characterization

In vitro evaluations of the prepared glucose biosensors were performed on the final glucose sensor. CV was performed different concentrations of glucose in PBS (0.01 M, pH = 7.4) at first to determine an appropriate working voltage (Fig. S3). To evaluate the biosensing performance, the modified biosensors were immersed in 13 mL of stirred PBS (0.01 M, pH = 7.4) for 10 min before the onset of successive injections (26 μL) of 1 M glucose solution. The sensitivities of the electrodes were measured after 1, 3, 5, 7 and 14 days with the same method over a two-week period. Glucose solution (1M), ascorbic acid solution (0.1 M), lactic acid solution (0.1 M), dopamine solution (0.1 M), uric acid solutions (50mM) and NaCl solution (0.1 M) were prepared before experiment (The same day of experiment). The specificity of the electrodes was tested in 13 mL of stirred PBS (0.01 M, pH = 7.4) by successively adding 26 μL of glucose solution, 26 μL of ascorbic acid solution, 26 μL of lactic acid solution, 52 μL of uric acid solution, 26 μL of NaCl solution and 26 μL of glucose solution to the same solution.

2.6 Biocompatibility test in vitro

Cytotoxicity was tested with the MTT test (detailed steps are listed in the supporting information). Cell adhesion tests were conducted with scanning electron microscopy (SEM) (detailed steps are listed in the supporting information).

2.7 In vivo experiment

The animal experiment is operated under the guide of laboratory animal center of Zhejiang university and we get the ethical approval from laboratory animal welfare ethics committee of Zhejiang university. In vivo experiments were conducted on Sprague–Dawley rats (weights in the range of 180 to 230 g) at the experimental animal center of the Zhejiang Province in Hangzhou, China, under anesthesia. The rats were anesthetized with 0.6 mL of pentobarbital sodium by injection. After the induction, the rats were immobilized on the operating table with tape to avoid body movements. The glucose biosensors were implanted under the skin in dorsal cervical areas. Before implantation, the dorsal cervical areas of the rats were shaved using depilatories, and the exposed skins were surgically cleaned with 2% chlorhexidine and alcohol. A circular skin incision (diameter of 3 - 5 mm) was made, and the sensor was implanted under the skin. The wound was protected by transparent dressings after operation. During the following 24 h, the rats were awakened, but were not allowed to eat for 12 h. Within this interval, ether anesthesia was administered by inhalation, and 0.6 mL of pentobarbital sodium was administered by injection to avoid violent grabbing. The sensor was then connected to an electrochemical workstation.

The sensor was allowed to operate for 1600 seconds to reach a stable state before the injection of 0.4 mL of glucose solution (wt. 50%) by intraperitoneal injection. During recording, we collected the blood by cutting a small wound in the toe and measured the blood glucose level using the ACCU-CHEK Performa. The total experimental time was approximately 2 h, and the rat was sacrificed by CO_2 after the experiment.

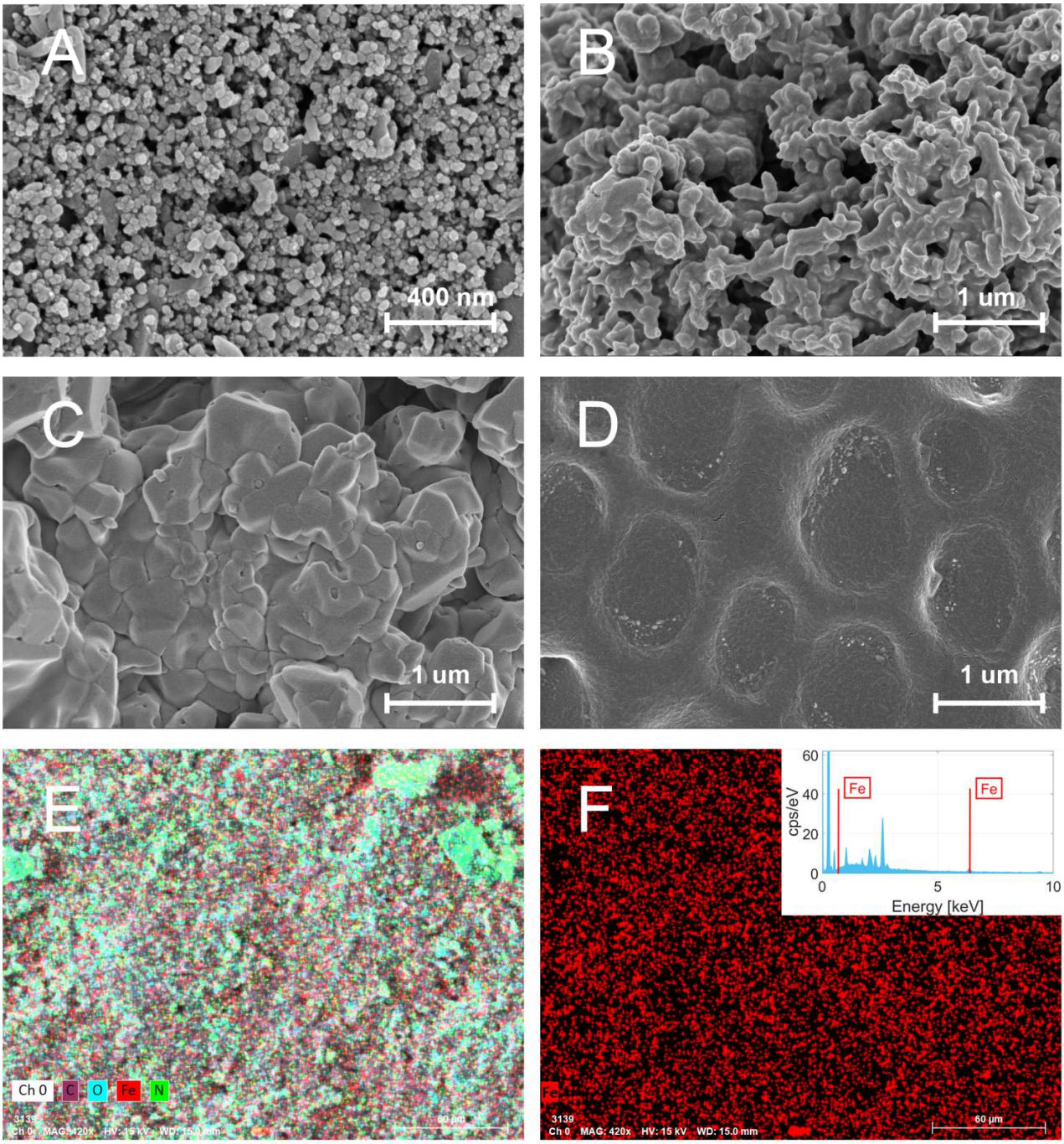

Fig. 2 Scanning electron microscopy (SEM) images of the glucose sensor. (A) Surface of the PANI nanostructure without the enzyme. (B) Nanostructured polyaniline (PANI)/glucose oxidase (GOD) enzyme intermixture. (C) Surface of the PANI/GOD nanostructure after crosslinking. (D) Polyurethane membranes. (E-F) EDS mapping: (E) EDS mapping includes C, O, Fe and N. (F) The same area of E that only shows Fe.

3. Results and discussion

3.1 Fabrication of glucose sensor

In this study, we developed a flexible double-sided, screen-printed electrode, which had a different structure from the traditional three-electrode structure (Fig. 1A). Twenty electrodes were screen-printed on a PET film, and were cut into independent, small electrode sizes (Fig. 1C). The electrode structure is simple, so electrodes can be potentially mass-produced with rapid prototyping. The electrode design was intentionally thin to ensure its suitability for implantable applications and detections (Kim et al. 2019; Ling et al. 2018). The screen-printed electrode was printed with PB-doped carbon ink that can directly decompose catalytically hydrogen peroxide. In this way, we did not need to modify the surface of the carbon-printed electrode with other catalytically active nanometal materials, such as nano-Pt or nano-Cu. PB was deposited on the surface of working electrode through printing carbon ink. The carbon ink doped with PB can catalytically decompose hydrogen peroxide. As shown in Fig. 2E and Fig. 2F, the energy-dispersive X-ray spectrum analysis confirmed the presence of iron, which is one of the components of PB. The carbon and nitrogen in the map should be from the substrate. In this way, a large amount of double-side screen-printed electrode used for glucose biosensor was able to be fabricated in a short time. The cost of single electrode was lowered and mass-production of glucose biosensor became easy.

To simplify the fabrication process and biosensor structure, we used a chemical instead of an electrochemical modification process. Therefore, the PANI was first chemically synthesized based on the mixture of an aqueous solution of aniline with ammonium persulphate. Single aniline molecules were polymerized in long-chain PANI with the oxidation of ammonium persulphate (Goto 2011). Through ultrasonication, the PANI chains formed nanostructures. Then the aqueous solution was dropped on the carbon electrode that resulted in the absorbance of the GOD enzyme (Fig. 2B). In most used methods, PANI was firstly modified on the surface of the electrode during the electrochemical process, and then adsorbed the GOD enzyme (Fang et al. 2014; Gaikwad et al. 2006). In comparison with these methods, the copolymerization of PANI and GOD enzyme formed a nanostructure. In this way, the GOD enzyme was tightly absorbed on the surface of the nano-PANI directly. Fig. 2A shows the nanostructure of PANI. Compared with the PANI fiber synthesized by the electrochemical process, the nano-PANI in our work was short and thick (Fang et al. 2017). The nano-PANI was less than 100 nm and was much shorter than the electro polymerized PANI. The nano-PANI increased the area of absorbing enzymes. During the mixing process, each PANI nanoparticle could adsorb enzymes instead of forming a three-dimensional (3D) network that may in turn increase the total amount of enzymes. In addition to physical adsorption, there are many amino groups in the PANI chains that could react with carboxyl groups on the side chains of the GOD enzyme (Pan et al. 2012). The two factors resulted in a better performance regarding enzyme immobilization. After crosslinking, glutaraldehyde covered the enzyme and linked with en-

zymes to form an integral structure (Fig. 2C). As shown in Fig. 2B, nano-PANI still have some bumps and branches. However, Fig. 2C showed that crosslinking with glutaraldehyde forms smooth polyhedrons. Thus, the structure of nano-PANI/GOD became more stable.

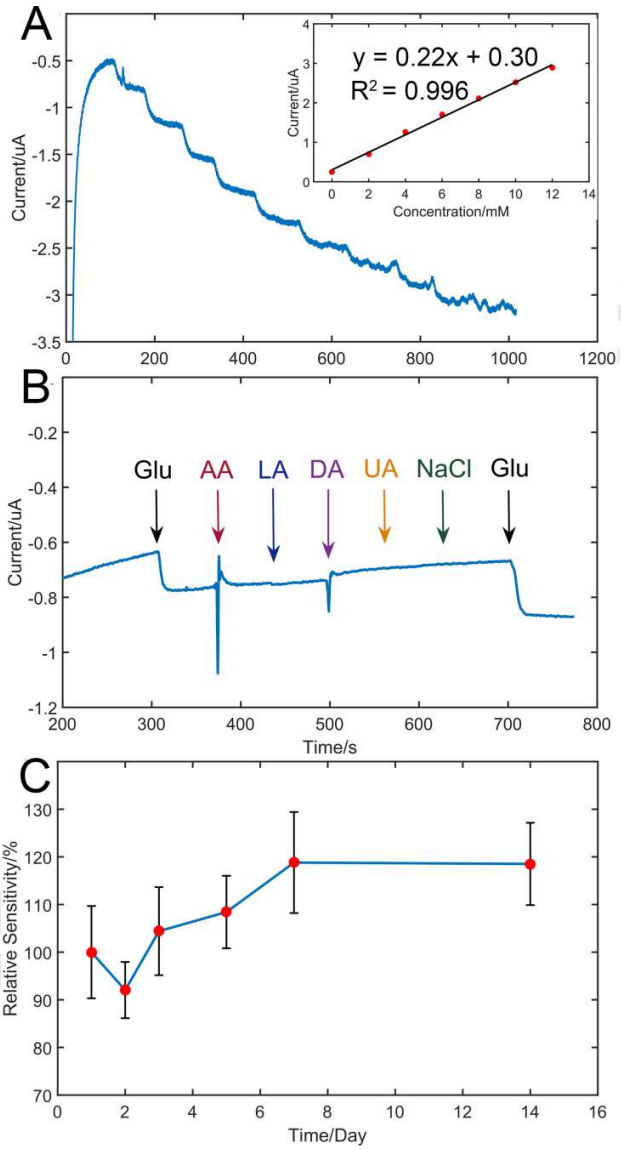

Fig. 3 Characterization of glucose biosensor. (A) Amperometric responses to glucose. (B) Amperometric responses to different interferences. (C) Relative sensitivity drift when the sensor is stored in PBS solution.

3.2 Characterization of glucose biosensor

CV showed that the E_{pa} of the scanning glucose was -0.3 V and the potential of $I_{pa}/2$ was 0 V. To achieve a broader linear range, the detection potential was selected as 0 V (Fig. S3). For sensing performance, the modified biosensors were immersed in 13 mL of PBS (0.01 M, pH = 7.4) and stirred for 10 min in the current–time experiment before the successive glucose solution injections (26 μL, 1 M)

subject to the applied potential of 0 V (potential of $I_{pa}/2$). The amperometric responses are shown in Fig. 3A. The reduction current increased gradually when a certain concentration of glucose was added to the PBS solution. The corresponding calibration curve is shown in Fig. 3A. According to the calibration curve, the sensitivity of the fabricated biosensor was 16.66 $\mu A \cdot mM^{-1} \cdot cm^{-2}$ (correlation coefficient R^2 = 0.9962). The amperometric response current showed a linear variation from 0 – 12 mM. Although the nano-PANI can increase the number of absorbed enzymes, the biosensors do not show a very high sensitivity toward glucose. The limiting diffusion of the PU layer may be the main reason. The amperometric response toward glucose and the linear range were worse than those for traditional metal needle electrodes given the poor conductivity of screen-printed electrodes (Fang et al. 2018). Nevertheless, this response was considered adequate for the detection of blood glucose.

The advantage of the biosensor is great specificity due to its low working voltage. The selectivity of the present glucose biosensor was studied by comparing the amperometric responses of physiological levels of various electroactive species. The amperometric response at different interference levels is shown in Fig. 3B. When firstly added glucose solution, the glucose biosensor gives an obvious response current. Then we added AA, LA, DA and UA solutions separately to figure out the glucose biosensor's response to these major interferences in blood. NaCl was also tested as ionic interference. The responses to these interferences were very small. Exactly, the prepared biosensor does not yield responses to LA, UA and NaCl. The amperometric responses after the injection of AA and DA became stable quickly. Finally, we added glucose solution again and the glucose biosensor gave a same response as before. It means that the glucose biosensor only reacts with glucose. A lower reaction voltage implies a less extensive reaction of active substances on the working electrode area, such as lactic and ascorbic acids (Ahmadalinezhad et al. 2009; Ricci and Palleschi 2005). However, the reaction of glucose was not affected due to the presence of PB that could catalytically reduce hydrogen peroxide at a very low voltage (E_{pa} = -0.3 V). In this study, the detection of glucose was performed at 0 V to reduce the interference from physiological species. This result shows that the biosensor printed with PB-doped carbon ink achieved enhanced specificity toward glucose.

The stability of the final glucose sensor was tested with the same sensitivity method every few days by storing it in PBS solution at 4°C, as shown in Fig. S4 (A - E). Fig. 3C shows the change of the average amperometric response of the final biosensor. As shown in Fig. 3C, the sensitivity of the biosensor increases as a function of the storage time. The amperometric responses toward glucose increase after 3 days. The main reason for the phenomenon is the fast degradation of the PU membranes that can potentially limit the diffusion of glucose. More glucose could pass through the diffusion limiting membrane so the sensitivity increased in the initial stage of the experiment (Henry et al. 2007; Wang et al. 2013).

After 1 week, the structure of the PU membrane became stable so the sensitivity of these biosensors did not change. As studied by Fang et al., the electrode coated with PU had longer stabilization time for about 2 weeks (Fang et al. 2017). However, the time of our electrodes was much shorter. In their study, they used PU/E-PU membrane. We used single layer of PU so the membrane became stable faster, which might be more helpful for obtaining a stable signal.

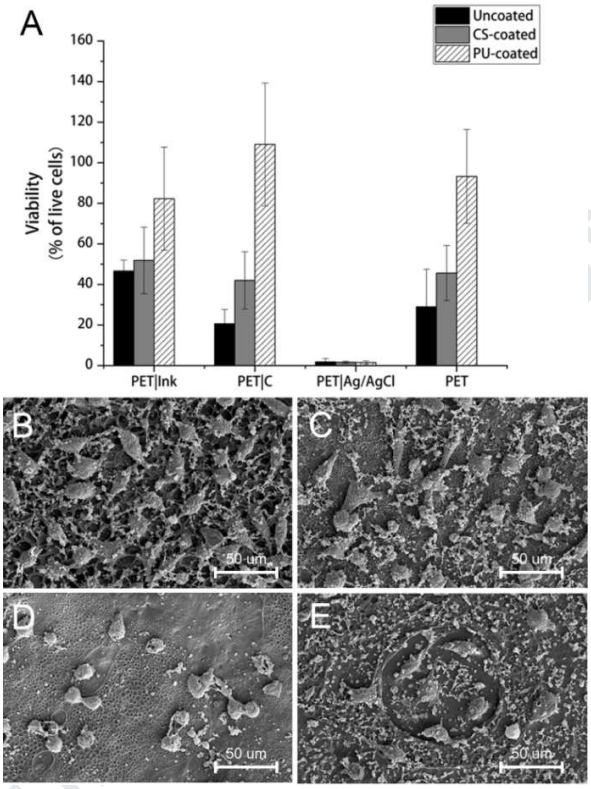

Fig. 4 (A) Cell viabilities of the four tested materials leaching liquor after cultures for 48h. 3 groups of PET substrate are printed with insulating ink (PET|ink), carbon ink (PET|C), Ag|AgCl (PET|Ag/AgCl). The fourth group of PET substrate is unprinted (PET). Each group is coated with chitosan (CS-coated), polyurethane (PU-coated) and uncoated. (B-E) SEM figures of cell adhesion on insulating ink, carbon ink, Ag/AgCl ink and PET substrates coated with polyurethane.

3.3 Evaluation of biocompatibility

The biocompatibility of biosensor materials was studied with cytotoxicity and cell adhesion tests. We evaluated the cytotoxicity via the MTT test following the addition of leaching liquor on these pads printed with different ink types coated with chitosan and polyurethane. The level of cell viability reflects the cytotoxicity of these materials (Atay et al. 2012; Lugscheider et al. 1994; Morales et al. 2014; Zhou et al. 2019). The cell viability could be calculated by the following formula:

$$Cell\ viability = (A - B) / B \times 100\% \quad (1)$$

Where A represents the absorption of the experimental group, and B represents the absorption of the blank control group. As shown in Fig. 4A, the pads were screen-printed with Ag/AgCl ink were as-

sociated with low-cell viabilities. These findings indicated that the Ag/AgCl ink might have higher cytotoxicity than other groups, even though it was coated with biocompatible materials. The other three materials had lower but almost the same cytotoxicity. As shown in Fig. S5 (A - D), the cell viability changes as a function of culture time. In every group, the pads coated with PU yielded the highest cell viabilities. The bare electrode exhibited a poor response in increasing cell viability but this could be improved when the electrode was coated. This phenomenon became more obvious as a function of culture time. The reason of this phenomenon may be attributed to the fact that coatings limit the diffusion of toxic particles released from substances. This explained the foundation of protective coatings.

The latex is the positive control and it should have the lowest cell viability because of its high cytotoxicity (Pariente et al. 2000). Nevertheless, latex had the highest viability in the Ag/AgCl group (Fig. S5D). This indicates again that the Ag/AgCl ink has a higher cytotoxicity than latex, and may not be suitable for implantation. This is because Ag^+ was highly cytotoxic even though coatings could limit the diffusion of Ag^+. A low Ag^+ concentration that diffused from the surface of the Ag/AgCl pads was adequate to kill the cells in this experiment.

The cell viability reached its maximum level after 24 h culture. This shows that the cells still have some resistance to toxic substances at the beginning of the experiment because there is an adequate quantity of nutrients in the culture medium, and cells proliferate faster. After the 24 h cultures, the number of cells increased but the nutrients left were inadequate and led to faster cell death rates compared with cell proliferation rates. Therefore, the number of cells decreased after 24 h.

In summary, biocompatible material coatings can partly decrease the cytotoxicity of screen-printed electrodes, especially in the cases of carbon and insulating inks. It will be better to replace the Ag/AgCl ink with other inks if the former is not necessary.

We then observed the morphologies of the cells after their cultures on pads screen-printed with different inks and coated with chitosan and PU, as shown in Fig. S6. The pads coated with biocompatible materials are more suitable for cell growth. This is because the coatings are smoother than bare pads. This makes cells attach more tightly on the surface of the pads. Seeded cells exhibit stretched cell morphology. As shown in Fig. S6 (D - F), spherical cells show that they do not grow well on the surface of Ag/AgCl pads. The chitosan and PU coatings can improve the surface morphology of the pads, but the high cytotoxicity of Ag/AgCl still kills most of the cells, while the remaining cells exhibit very poor morphologies. The results showed that substrate materials also affected the growth of cells. These findings are consistent with MTT test.

There is no doubt that chitosan and PU are beneficial in improving cells growth. However, outcomes based on cytotoxicity tests and SEM observations are opposite to what was expected. It seems

that the PU coating could increase cell viability because it has a limiting diffusion pertaining toxic substances, but the SEM observation showed that the chitosan coating leads to an increased cell number and better morphologies (Kalyoncuoglu et al. 2018). This contradiction is attributed to the degradation and hydrophobicity of PU. The PU surface has some lipid groups that are hydrophobic, but the surface of chitosan is hydrophilic (Kim and Masuoka 2009). In addition, the degradation of PU makes the surface of the PU coating uneven. The two disadvantages make the PU coating unsuitable for cell growth. However, the PU has a better diffusion limit than chitosan. The leaching liquor of PU coating contains fewer toxic substances than chitosan coating. This explains the cytotoxicity test outcomes. If all the effects are taken into consideration, the choice of PU as the biocompatible layer is justified.

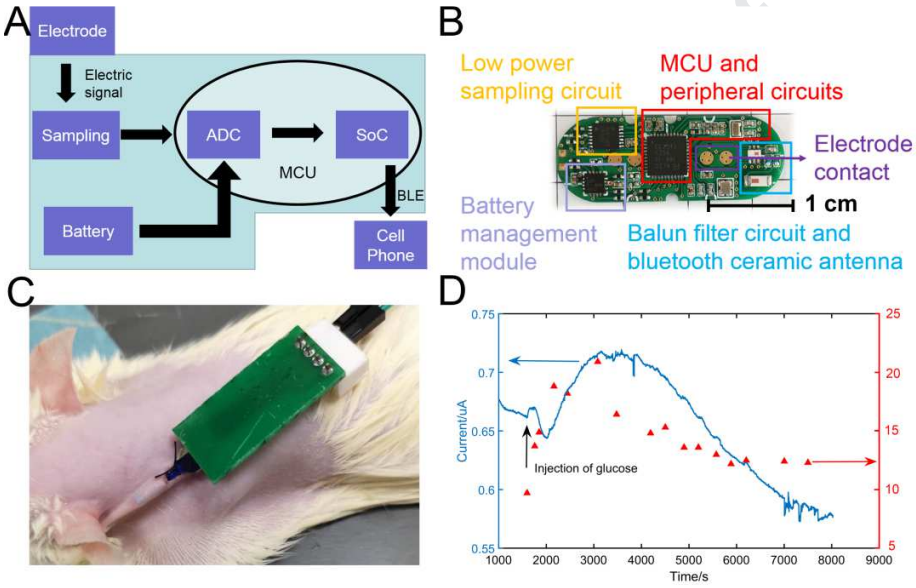

Fig. 5 (A) Block diagram of collector. Analog-to-Digital Converter (ADC) and System-on-a-chip (SoC) are integrated in one microcontroller unit (MCU). Bluetooth low energy (BLE) interacts with smart phone via the Bluetooth 4.0. (B) Circuit diagram of collector. (C-D) Response of biosensor toward the injection of glucose (blue line) and real-time blood glucose level measured by the AUCC-CHEK Performa from samples extracted from the paws (red scatter plot).

3.4 In vivo glucose level monitoring

We designed a collector to sample, process, and transmit the electric signal form our glucose sensor (Fig. 5A and Fig. 5B). A low-power sampling circuit can collect the electrode current and convert the analog signal to a digital form. The signal can be simply processed and transmitted to our cell phone by a Bluetooth ceramic antenna. The entire system is powered with a 45 mA·h lithium battery and can (theoretically) work for at least 14 days.

During the vivo experiments, the rats were anesthetized with pentobarbital sodium, and the sensor was implanted under the skin in dorsal cervical areas (Fig. 5C). The sensor was stabilized in vivo for 24 h before amperometric recordings. The recordings were conducted with the IVIUM CompacStat.h elec-

trochemical workstation for increased accuracy at a 0 V potential. Fig. 5D shows the current–time response and blood glucose levels as measured by the AUCC-CHEK Performa. Before testing, the rats were forbidden to eat for 12 h to stabilize their blood glucose levels. The biosensor was allowed to stabilize for approximately 2 h before testing. After the injection of0.4mL of glucose solution (wt. 50%) through the abdominal cavity at ~1600s, the blood glucose level increased immediately and reached its maximum value ~20 min later. The blood glucose levels returned to baseline after ~1 h. The trend of the blood glucose was different when injections were performed with caudal vein catheters (Fang et al. 2018) because the intraperitoneal absorption was relatively slower than the intravenous injection, and the process lasted for a longer time.

The recording data from the sensor was compared to the blood glucose level. The sensor data yielded almost the same blood glucose level trend with a noted delay of ~10 min. This phenomenon is attributed to the fact that the biosensor measures the glucose in the interstitial fluid rather than blood. There is a 5 - 10 min delay until the time effective tissue fluid change occur, which is consistent with other studies (Fang et al. 2014; Fang et al. 2018). Meanwhile, the glucose level in the tissue fluid is lower than that of blood that results in a lower current response in vivo. However, the response of the sensor declines continually when the blood glucose level becomes stable and lasts longer compared with the blood glucose levels. This may be attributed to the instability of the sensor itself and the low-diffusion rate in the interstitial tissue fluid. Complex internal environment components and foreign body response (FBR) also lead to a faster degradation in the sensor performance compared with its in vitro response (Morais et al. 2010). Another possible reason for the drift after ~6000 s is short polarization time of the electrode. This electrode had not been reached equilibrium in such a short time.

4. Conclusions

In this study, we developed a CGMS with a flexible double-sided screen-printed electrode. The PB-doped carbon ink and nano-PANI/GOD mixture immobilizations were introduced in the implantable glucose biosensor. Flexible double-sided, screen-printed electrodes are more suitable for implantation, and they ease user pain. The PB-doped carbon ink can directly catalyze the reduction of hydrogen peroxides, makes it possible to detect glucose at a low voltage, and thus decreases the interference from physiological species. The nano-PANI/GOD mixture increased the area of absorbing glucose. The in vitro experiment proved the long lifespan of the biosensor and its enhanced specificity toward glucose. Cytotoxicity evaluation explored the cytotoxicity of all the materials we used in the electrodes. The results of the MTT test and the SEM observations showed good PU biocompatibility. The in vivo experiments showed that the CGMS could detect glucose levels in rats. Through these improvements, we low-

er the cost of glucose biosensor for CGMS and simplify the fabrication process. It is helpful for large-scale production. A delicate quantitative analysis for biocompatibility of materials in the biosensor was given to guarantee safe use for implantation. However, the CGMS still needs some improvements in linearity and long-time stability in vivo. Our future work will focus on the enhancements of the sensitivity and linear range of the glucose biosensor. In vivo measurements should be optimized for stability and sensitivity in consideration of the disparities of the physiological environment of interstitial tissue fluid. Our previous works have applied PLAG, E-PU and zwitterionic materials in protective layer to improve in vivo performance of glucose biosensors. Additionally, the FBR also plays a significant role in the performance of the implantable biosensor, and its impact on the biosensor requires further study (Gray et al. 2019; Morais et al. 2010).

Role of the Funding Source

The work was supported by the Natural Science Foundation of Zhejiang Province [grant numbers LQ20F010011 and LY18H180006], the Key Research and Development Program of Zhejiang Province [grant number 2019C03066], and the National Natural Science Foundation of China [grant numbers 61501400 and 81501555].

Acknowledgements

We are thankful for the help received from the staff members of the Frozen Electron Microscope Center of Zhejiang University. The in vivo experiments were conducted with the guidance of Ke Wu, a Ph.D. candidate of the Medical College of Zhejiang University.

References

Ahmadalinezhad, A., Kafi, A.K.M., Chen, A.C., 2009. Electrochemistry Communications 11(10), 2048-2051.

Atay, A., Bozok Cetintas, V., Cal, E., Kosova, B., Kesercioglu, A., Guneri, P., 2012. Dent. Mater. J. 31(6), 1082-1086.

Cinti, S., Cusenza, R., Moscone, D., Arduini, F., 2018. Talanta 187, 59-64.

Fang, L., Liang, B., Yang, G., Hu, Y., Zhu, Q., Ye, X., 2014. Biosens. Bioelectron. 56, 91-96.

Fang, L., Liang, B., Yang, G., Hu, Y., Zhu, Q., Ye, X., 2017. Biosens. Bioelectron. 97, 196-202.

Fang, Y., Wang, S., Liu, Y., Xu, Z., Zhang, K., Guo, Y., 2018. Biosens. Bioelectron. 110, 44-51.

Gaikwad, P.D., Shirale, D.J., Gade, V.K., Savale, P.A., Kharat, H.J., Kakde, K.P., Shirsat, M.D., 2006. Int J Electrochem Sc 1(8), 425-434.

Goto, H., 2011. Fibres Text East Eur 19(2), 15-17.

Gray, M.E., Meehan, J., Blair, E.O., Ward, C., Langdon, S.P., Morrison, L.R., Marland, J.R.K., Tsiamis, A., Kunkler, I.H., Murray, A., Argyle, D., 2019. J. Biomed. Mater. Res. B Appl. Biomater. 107(5), 1620-1633.

He, W.S., Sun, Y.M., Xi, J.B., Abdurhman, A.A.M., Ren, J.H., Duan, H.W., 2016. Anal. Chim. Acta 903, 61-68.

Henry, J.A., Simonet, M., Pandit, A., Neuenschwander, P., 2007. Journal of Biomedical Materials Research Part A 82a(3), 669-679.

Kalyoncuoglu, U.T., Yilmaz, B., Koc, S.G., Evis, Z., Arpaci, P.U., Kansu, G., 2018. Clin. Implant Dent. Relat. Res. 20(6), 1022-1029.
Karyakin, A.A., Karyakina, E.E., Gorton, L., 2000. Anal. Chem. 72(7), 1720-1723.
Kausar, A., 2019. Mater. Res. Innovations 24(2), 113-122.
Kim, K.B., Choi, H., Jung, H.J., Oh, Y.J., Cho, C.H., Min, J.H., Yoon, S., Kim, J., Cho, S.J., Cha, H.J., 2019. Biosens. Bioelectron. 143, 111622.
Kim, M.C., Masuoka, T., 2009. Appl. Surf. Sci. 255(8), 4684-4688.
Kwak, Y.H., Choi, D.S., Kim, Y.N., Kim, H., Yoon, D.H., Ahn, S.S., Yang, J.W., Yang, W.S., Seo, S., 2012. Biosens. Bioelectron. 37(1), 82-87.
Liang, B., Fang, L., Yang, G., Hu, Y., Guo, X., Ye, X., 2013. Biosens. Bioelectron. 43, 131-136.
Ling, W., Liew, G., Li, Y., Hao, Y., Pan, H., Wang, H., Ning, B., Xu, H., Huang, X., 2018. Adv. Mater. 30(23), e1800917.
Lugscheider, E., Knepper, M., Heimberg, B., Dekker, A., Kirkpatrick, C.J., 1994. J Mater Sci-Mater M 5(6-7), 371-375.
Morais, J.M., Papadimitrakopoulos, F., Burgess, D.J., 2010. AAPS J 12(2), 188-196.
Morales, J.M.H., Souriau, J.C., Ratel, D., Berger, F., Simon, G., 2014. Elec Comp C, 478-483.
Nguyen, T.N.H., Nolan, J.K., Park, H., Lam, S., Fattah, M., Page, J.C., Joe, H.E., Jun, M.B.G., Lee, H., Kim, S.J., Shi, R., Lee, H., 2019. Biosens. Bioelectron. 131, 257-266.
Nossol, E., Zarbin, A.J.G., 2009. Adv. Funct. Mater. 19(24), 3980-3986.
Pan, L.J., Yu, G.H., Zhai, D.Y., Lee, H.R., Zhao, W.T., Liu, N., Wang, H.L., Tee, B.C.K., Shi, Y., Cui, Y., Bao, Z.N., 2012. P Natl Acad Sci USA 109(24), 9287-9292.
Pariente, J.L., Bordenave, L., Jacob, F., Bareille, R., Baquey, C., Le Guillou, M., 2000. Eur. Urol. 38(5), 640-643.
Ricci, F., Palleschi, G., 2005. Biosens. Bioelectron. 21(3), 389-407.
Shin, J.H., Marxer, S.M., Schoenfisch, M.H., 2004. Anal. Chem. 76(15), 4543-4549.
Shoaie, N., Daneshpour, M., Azimzadeh, M., Mahshid, S., Khoshfetrat, S.M., Jahanpeyma, F., Gholaminejad, A., Omidfar, K., Foruzandeh, M., 2019. Microchimica Acta 186(7).
Wang, J., 2008. Chem. Rev. 108(2), 814-825.
Wang, N., Burugapalli, K., Song, W.H., Halls, J., Moussy, F., Ray, A., Zheng, Y.D., 2013. Biomaterials 34(4), 888-901.
Xu, W., He, J., Gao, L., Zhang, J., Hui, J., Guo, Y., Li, W., Yu, C., 2015. Journal of Electroanalytical Chemistry 741, 8-13.
Yoo, E.H., Lee, S.Y., 2010. Sensors 10(5), 4558-4576.
Yu, B., Long, N., Moussy, Y., Moussy, F., 2006. Biosens. Bioelectron. 21(12), 2275-2282.
Zeng, Q., Cheng, J.S., Liu, X.F., Bai, H.T., Jiang, J.H., 2011. Biosens. Bioelectron. 26(8), 3456-3463.
Zhang, D., Zhang, K., Yao, Y.L., Xia, X.H., Chen, H.Y., 2004. Langmuir 20(17), 7303-7307.
Zhou, J., Ma, Z., Hong, X., Wu, H.M., Ma, S.Y., Li, Y., Chen, D.J., Yu, H.Y., Huang, X.J., 2019. ACS Sensors 4(4), 931-937.

Highlights

- A new design of flexible biosensor for continuous glucose monitoring with double-side screen-printed electrode.
- Suitable for large-scale fabrication achieved by single-step modification of nano-polyaniline and glucose oxidase.
- Excellent specificity towards glucose using Prussian blue doped carbon ink.
- Quantitative cytotoxicity evaluation of the entire biosensor through MTT test.

Declaration of interest statements

The authors declare that they have no known competing financial interests or personal relationships that could have appeared to influence the work reported in this paper.